Non-pore lining amino acid side chains influence anion selectivity of the human CFTR Cl^- channel expressed in mammalian cell lines

Paul Linsdell, Shu-Xian Zheng and John W. Hanrahan

Department of Physiology, McGill University, Montréal, Québec, Canada H3G 1Y6

(Received 26 March 1998; accepted after revision 3 July 1998)

1. The effects of individually mutating two adjacent threonine residues in the sixth membrane-spanning region (TM6) of the cystic fibrosis transmembrane conductance regulator (CFTR) Cl^- channel on permeation properties were examined using patch clamp recording from mammalian cell lines stably expressing human CFTR.

2. A number of mutations of T338 significantly affected the permeation properties of the channel. Increases and decreases in single channel conductance were observed for different mutants. Anion selectivity was strongly affected, with no two channel variants sharing the same selectivity sequence. Several mutations led to strong inward rectification of the macroscopic current–voltage relationship. The effects of these mutations on permeation properties were correlated with the size of the amino acid side chain substituted, rather than its chemical nature.

3. Most mutations of T339 resulted in a lack of functional channel expression and apparent misprocessing of the protein. One mutant, T339V, was characterized in detail; its permeation properties were significantly altered, although these effects were not as strong as for T338 mutations.

4. These results suggest an important role for T338 in controlling the permeation properties of the CFTR Cl^- channel. It is suggested that mutation of this residue alters the interaction between permeating anions and the channel pore via an indirect effect on the orientation of the TM6 helix.

Cystic fibrosis (CF) is caused by mutations in a single gene, that encoding the cystic fibrosis transmembrane conductance regulator (CFTR; Riordan *et al.* 1989). CFTR is a member of the 'ATP-binding cassette' superfamily of membrane transport proteins, which forms an ion channel permeable both to Cl^- (Gadsby *et al.* 1995; Hanrahan *et al.* 1995) and to large intracellular organic anions (Linsdell & Hanrahan, 1998).

Alteration of anion selectivity following site-directed mutagenesis of CFTR provided key evidence that CFTR itself forms a Cl^- channel (Anderson *et al.* 1991). However, although numerous mutations have since been shown to alter CFTR permeation properties such as single channel conductance (Sheppard *et al.* 1993; Tabcharani *et al.* 1993; McDonough *et al.* 1994; Sheppard *et al.* 1996; Linsdell *et al.* 1997*b*) and interaction with channel blockers (Tabcharani *et al.* 1993; McDonough *et al.* 1994; Linsdell & Hanrahan, 1996), only modest alterations of anion selectivity have been reported after mutagenesis (e.g. Anderson *et al.* 1991; Linsdell *et al.* 1997*b*; Mansoura *et al.* 1998), and the molecular determinants of CFTR anion selectivity remain unknown. Wild-type CFTR shows a lyotropic or 'weak field strength' anion selectivity sequence (Linsdell *et al.* 1997*b*; Tabcharani *et al.* 1997; Linsdell & Hanrahan, 1998), similar to that observed in most Cl^- channels that have been studied in detail, e.g. γ-aminobutyric acid and glycine receptors (Bormann *et al.* 1987; Fatima-Shad & Barry, 1993), epithelial outwardly rectifying Cl^- channels (Li *et al.* 1990; Halm & Frizzell, 1992) and volume-regulated Cl^- channels (Arreola *et al.* 1995; Jackson *et al.* 1996). This similarity suggests that the mechanism of anion selectivity may be conserved between different Cl^- channel types. However, the physical basis of lyotropic anion selectivity has not yet been identified in any Cl^- channel.

Previously, we reported that a double amino acid substitution in the sixth membrane-spanning region (TM6) of CFTR, TT338,339AA, significantly increased channel conductance and also increased permeability to several large anions (Linsdell *et al.* 1997*b*). However, interpretation of these results was complicated by the demonstration, using substituted cysteine accessibility mutagenesis, that neither of these amino acids have side chains which are accessible to the aqueous lumen of the pore (Cheung & Akabas, 1996). Here we report the functional effects of mutating these threonine residues individually to amino acids of different side chain size and polarity. The implications of this work for

the structure of the CFTR pore and for the mechanism of anion selectivity are discussed.

Some of these results have been reported in abstract form (Linsdell *et al.* 1997*c*).

METHODS

CFTR mutagenesis and expression

Site-directed mutagenesis of human CFTR cDNA was carried out using the polymerase chain reaction (PCR) with Vent polymerase (New England Biolabs, Mississauga, Ontario, Canada). Use of partially degenerate PCR primers allowed substitution of several different amino acids at the same site. PCR fragments were subcloned into pNUT–CFTR (Tabcharani *et al.* 1991) before being screened by DNA sequencing of the entire inserted region, using the T7 polymerase sequencing kit (United States Biochemical, Cleveland, OH, USA). pNUT–CFTR clones containing mutations of interest were transfected into subconfluent baby hamster kidney (BHK) and Chinese hamster ovary (CHO) cells using calcium phosphate co-precipitation, as described previously (Seibert *et al.* 1996). Individual stably transfected colonies were selected using methotrexate (MTX; 50 μM for CHO cells, and 500 μM for BHK cells). CFTR protein expression was confirmed by Western blot analysis using an anti-CFTR antibody (M3A7) as described previously (Chang *et al.* 1993; Seibert *et al.* 1996). For immunoprecipitation of CFTR (Fig. 1*E*), total protein was extracted from the cell lysate by centrifugation, and pre-incubated with 2 μg ml^{-1} M3A7 antibody overnight. CFTR–M3A7 complex was then purified using Protein G-coated sepharose beads (Sigma) and analysed using Western blotting.

Electrophysiological recordings

Macroscopic and single channel CFTR current recordings were both made using the excised, inside-out configuration of the patch clamp technique, as described previously (Linsdell & Hanrahan, 1996, 1998; Linsdell *et al.* 1997*a*). BHK cells were used for macroscopic recordings and CHO cells for single channel recordings (Linsdell & Hanrahan, 1998), except where indicated in the text. Channels were activated following patch excision by exposure of the cytoplasmic face of the patch to 40–180 nM protein kinase A catalytic subunit (PKA; prepared in the laboratory of Dr M. P. Walsh, University of Calgary, Alberta, Canada, as described previously; Tabcharani *et al.* 1991) plus 1 mM MgATP (Sigma). All macroscopic current–voltage relationships shown have had the background (leak) current recorded before addition of PKA subtracted digitally as described previously (Linsdell & Hanrahan, 1996, 1998). Current traces were filtered at 100 Hz (for macroscopic currents) or 50 Hz (for single channel currents) using an 8-pole Bessel filter, digitized at 250 Hz and analysed using pCLAMP 6 computer software (Axon Instruments). Current traces for variance analysis (see below) were filtered at 500 Hz and digitized at 1 kHz.

Solutions contained (mM): 150 NaCl, 2 $MgCl_2$, 10 Tes; or 154 NaX (where X is the anion being tested; see Table 1 for a list of anions used), 2 $Mg(OH)_2$, 10 Tes; solutions were adjusted to pH 7·4 with NaOH. Where the pipette solution did not contain Cl^- (Fig. 9), the Ag–AgCl wire inside the pipette was protected by a NaCl-containing agar bridge. Given voltages have been corrected for measured liquid junction potentials of up to 12 mV existing between dissimilar pipette and bath solutions. All chemicals were obtained from Sigma, except $NaClO_4$, $NaPF_6$, sodium benzoate and sodium methane sulphonate (Aldrich, Milwaukee, WI, USA). Experiments with different anions were carried out on different patches.

Macroscopic current–voltage relationships were constructed using depolarizing voltage ramp protocols, with a rate of change of voltage of 37·5–100 mV s^{-1} (see Linsdell & Hanrahan, 1996, 1998). All macroscopic current–voltage relationships shown are the mean of at least three consecutive ramps, applied at 10 s intervals. The current reversal potential, V_{rev}, was estimated by fitting a polynomial function to the current–voltage relationship, and was used to estimate the permeability of different anions relative to that of chloride (P_X/P_{Cl}) according to the equation:

$$P_X/P_{Cl} = \exp(\Delta V_{rev} F/RT), \quad (1)$$

where ΔV_{rev} is the difference between the reversal potential observed under biionic conditions with a test anion X^- and that observed with symmetrical Cl^-, and F, R and T have their usual thermodynamic meanings.

The functional diameter of the narrowest part of the pore (Figs 8 and 9) was estimated by modelling the pore as a cylinder permeated by cylindrical-shaped ions, as described previously (Linsdell *et al.* 1997*b*; Linsdell & Hanrahan, 1998). Permeability ratios were related to ion diameter according to an 'excluded volume effect' (Dwyer *et al.* 1980):

$$P_X/P_{Cl} = k(1 - (a/d))^2, \quad (2)$$

where a is the unhydrated diameter of the ion (estimated as described previously; Linsdell & Hanrahan, 1998), d is the diameter of the pore, and k is a proportionality constant.

Measurements of macroscopic current variance (Fig. 5) were made during the slow activation of macroscopic current by low concentrations of PKA (approximately 40 nM) as described previously (Linsdell & Hanrahan, 1998). Mean current and current variance were calculated for 5 s subrecords filtered at 500 Hz, giving a bandwidth of 0·2–500 Hz. The length of subrecords was chosen to minimize the error due to current activation during each subrecord without omitting too much of the low frequency variance. Variance *versus* mean current relationships were fitted by the equation:

$$\sigma_I^2 = iI - (I^2/N), \quad (3)$$

where σ_I^2 is the current variance, I is the mean current, i is the unitary current and N is the total number of channels.

Experiments were carried out at room temperature (20–23 °C). Throughout, values are given as means ± S.E.M. For graphical presentation of mean values, error bars represent ± S.E.M.; where no error bar is shown, it is smaller than the size of the symbol.

RESULTS

Expression and processing of CFTR mutants

The CFTR molecule consists of twelve membrane-spanning regions, two cytoplasmic nucleotide binding domains (NBDs), and a cytoplasmic regulatory (R) domain (Fig. 1*A*; Riordan *et al.* 1989). We made a number of single amino acid substitutions for residues T338 and T339 within the TM6 region (Fig. 1*B*). Stable expression of all six T338 mutants constructed in BHK cells led to the production of both core-glycosylated (band B) and fully glycosylated (band C) CFTR protein, although some mutants (especially T338F)

consistently made less band C protein than wild-type (Fig. 1*C*). In contrast, of five mutations made at T339, only one (T339V) produced detectable levels of CFTR protein in Western blots using cell lysates from one confluent 10 cm culture plate (approximately 2×10^6–3×10^6 cells; Fig. 1*D*). However, following immunoprecipitation of CFTR protein from five confluent plates, a very small amount of T339S mutant CFTR protein was detectable by Western blotting (Fig. 1*E*), indicating that the BHK cells had been successfully transfected with the mutated plasmid, but that most mutations at T339 caused more severe misprocessing and/or degradation of the CFTR protein.

Chloride permeation in T338 mutants

Expression of wild-type and T338 mutant CFTR Cl^- channels in BHK cells led to the appearance of macroscopic PKA- and ATP-dependent Cl^- currents in inside-out membrane patches (Fig. 2; Linsdell & Hanrahan, 1996). In contrast, no currents were activated under these conditions in large inside-out patches excised from BHK cells expressing T338F ($n = 8$; not shown). As expected, wild-type CFTR showed a linear current–voltage relationship under these symmetrical (154 mM Cl^-) ionic conditions. In contrast, several T338 mutants showed marked inward current rectification under these conditions (Fig. 2). This rectification was quantified by comparing the outward

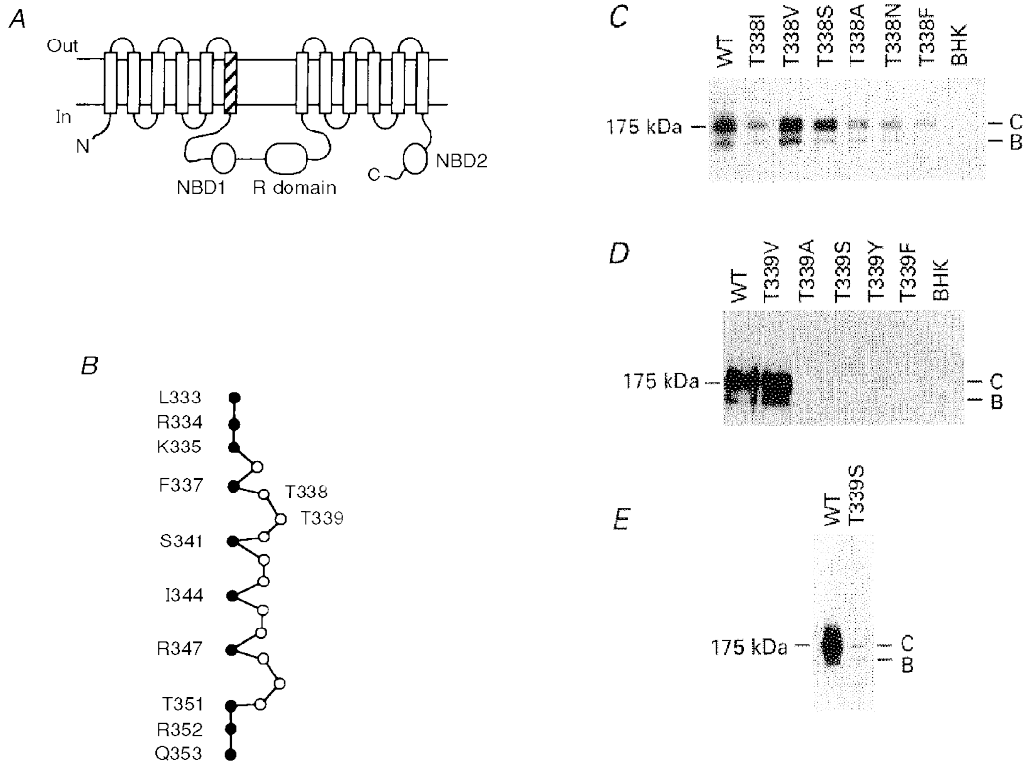

Figure 1. Structure of the TM6 region of CFTR

A, proposed overall topology of CFTR (as described by Riordan *et al.* 1989), comprising twelve membrane-spanning regions, two cytoplasmic nucleotide binding domains (NBDs) and the cytoplasmic regulatory (R) domain. The hatched area indicates TM6. N, N-terminus; C, C-terminus. *B*, primary sequence of TM6, after Cheung & Akabas (1996). Filled circles indicate those amino acids with side chains which have been proposed, on the basis of substituted cysteine accessibility mutagenesis, to line the aqueous lumen of the pore. According to this criterion, it has been proposed that neither T338 nor T339 have lumen-accessible side chains (Cheung & Akabas, 1996). *C*, immunoblots of T338 mutants stably expressed in BHK cells, carried out as described previously (Chang *et al.* 1993; Seibert *et al.* 1996). Equal amounts of total cellular protein were used in each lane. No CFTR protein was detected in untransfected cells (BHK, right-hand lane). Here and in *D* and *E*, the position of maltose binding protein–β-galactosidase from *Escherichia coli* (175 kDa marker) is shown on the left. Molecular mass markers below 100 kDa are not shown. WT, wild-type; B, core-glycosylated CFTR protein; C, fully glycosylated CFTR protein. *D*, immunoblots of T339 mutants stably expressed in BHK cells. Data shown are representative of at least ten experiments on different BHK cell colonies for each T339 mutant, over a total of four transfections for each mutant. *E*, Western blot of immunoprecipitated T339S protein, carried out as described in Methods. Similar results were observed with T339A, T339Y and T339F (not shown).

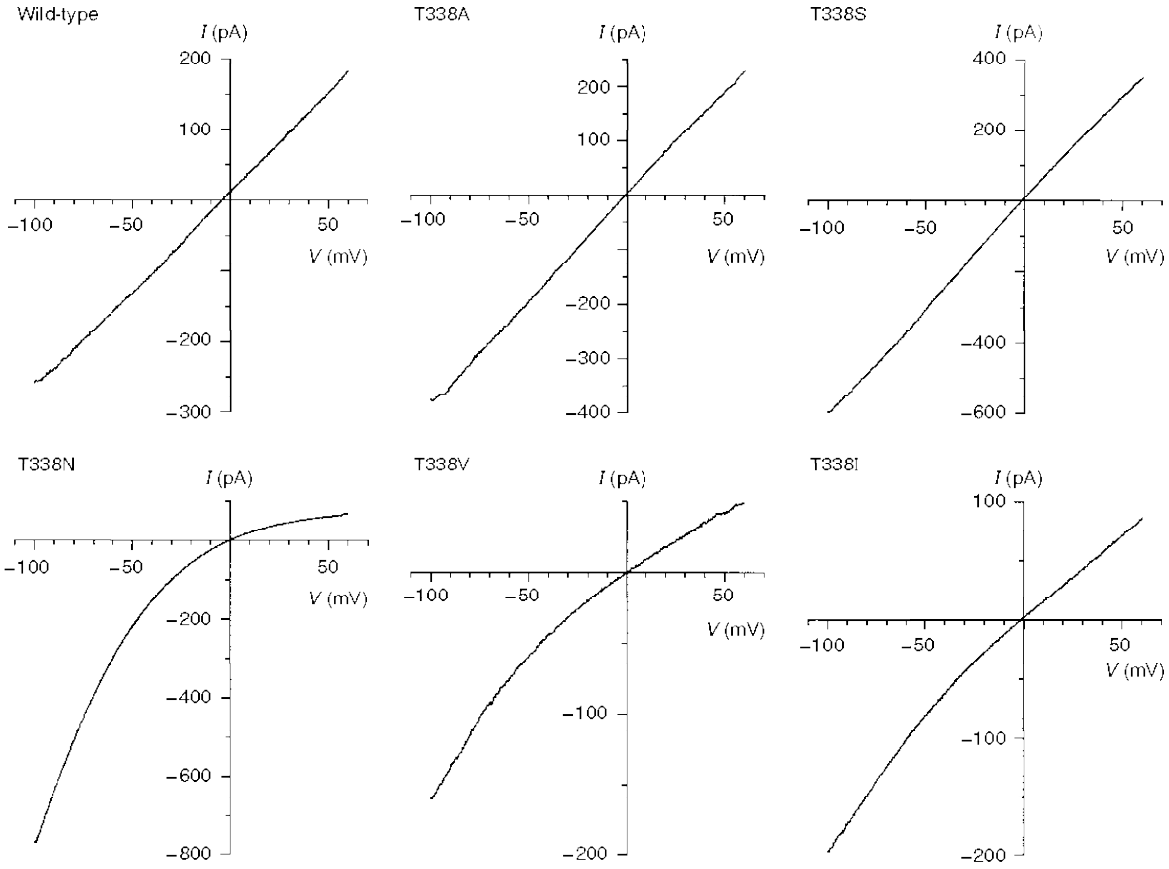

Figure 2. Example macroscopic current–voltage relationships for wild-type and T338 mutant CFTRs, recorded with symmetrical Cl^--containing solutions

Note the inward rectification observed with some T338 mutants, especially T338N. Patches were held at 0 mV and depolarizing voltage ramps were applied at a rate of 100 mV s^{-1}. Current–voltage relationships were leak subtracted as described in Methods.

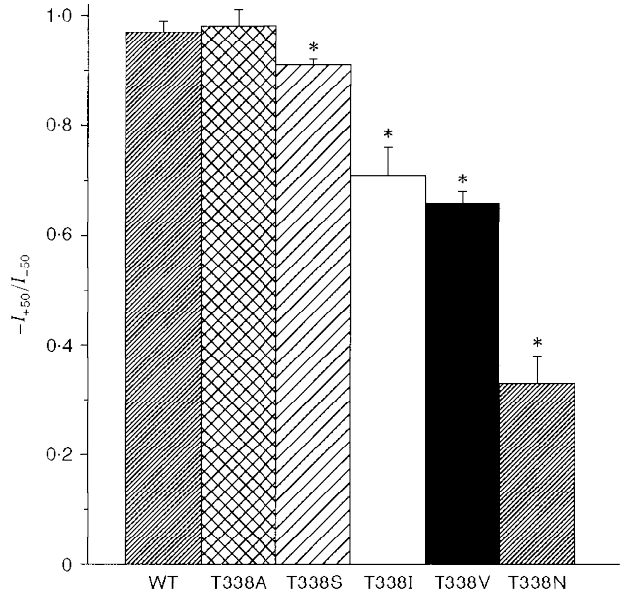

Figure 3. T338 mutants show significant inward rectification under symmetrical ionic conditions

Asterisks indicate a mean ratio of outward current amplitude at +50 mV (I_{+50}) to inward current amplitude at −50 mV (I_{-50}) significantly less than one ($P < 0{\cdot}05$, Student's two-tailed t test). Means + S.E.M. of data from twenty-six patches for wild-type and three to six patches for T338 mutants.

current amplitude at +50 mV (I_{+50}) with the inward current amplitude at −50 mV (I_{-50}) (Fig. 3). Significant rectification resulting in a $-I_{+50}/I_{-50}$ ratio significantly less than one was observed in all mutants except T338A (Fig. 3). Rectification was particularly strong in T338N ($-I_{+50}/I_{-50} = 0{\cdot}33 \pm 0{\cdot}05$; $n = 6$).

Single CFTR channel currents in inside-out patches excised from CHO cells stably expressing wild-type, T338A or T338S are shown in Fig. 4*A*. However, clear single channel currents were never resolved for T338N, T338V or T338I, either in CHO cell patches or in patches excised from BHK cells selected using a lower concentration of MTX (20 μM), at potentials as hyperpolarized as −100 mV (data not shown). This suggests that each of these mutants might carry unitary currents too small to resolve using single channel recording. Mean single channel current–voltage relationships for those channel variants that could be resolved are shown in Fig. 4*B* and *C*. Mean slope conductance was increased from $7{\cdot}9 \pm 0{\cdot}1$ pS ($n = 18$) for wild-type to $10{\cdot}4 \pm 0{\cdot}1$ pS ($n = 9$) for T338A and $11{\cdot}3 \pm 0{\cdot}2$ pS ($n = 5$) for T338S. This represents a significant increase in conductance compared with wild-type for both of these mutants ($P < 0{\cdot}001$; Student's two-tailed t test). Although the gating of T338A and T338S channels was not studied in detail, no striking differences from wild-type were noted. As with wild-type, the open probability of both of these mutants was time and voltage independent.

We attempted to make some estimate of the conductance of T338N, T338V and T338I channels by analysing the increase in current noise associated with macroscopic current activation (Fig. 5). We have previously used this technique to estimate the amplitude of unitary currents carried by large anions through CFTR (Linsdell & Hanrahan, 1998). Activation of wild-type CFTR at −50 mV was associated with a clear increase in noise (Fig. 5*A*). The relationship between Cl^- current amplitude and current variance (Fig. 5*B*) gave an estimate of the unitary current, i, of $0{\cdot}26 \pm 0{\cdot}06$ pA ($n = 5$), suggesting a chord conductance of $5{\cdot}27 \pm 1{\cdot}10$ pS ($n = 5$) at −50 mV. This estimate is somewhat lower than the value measured directly by single channel recording (7·9 pS; see above), suggesting that part of the CFTR-associated current noise may be lost during recording.

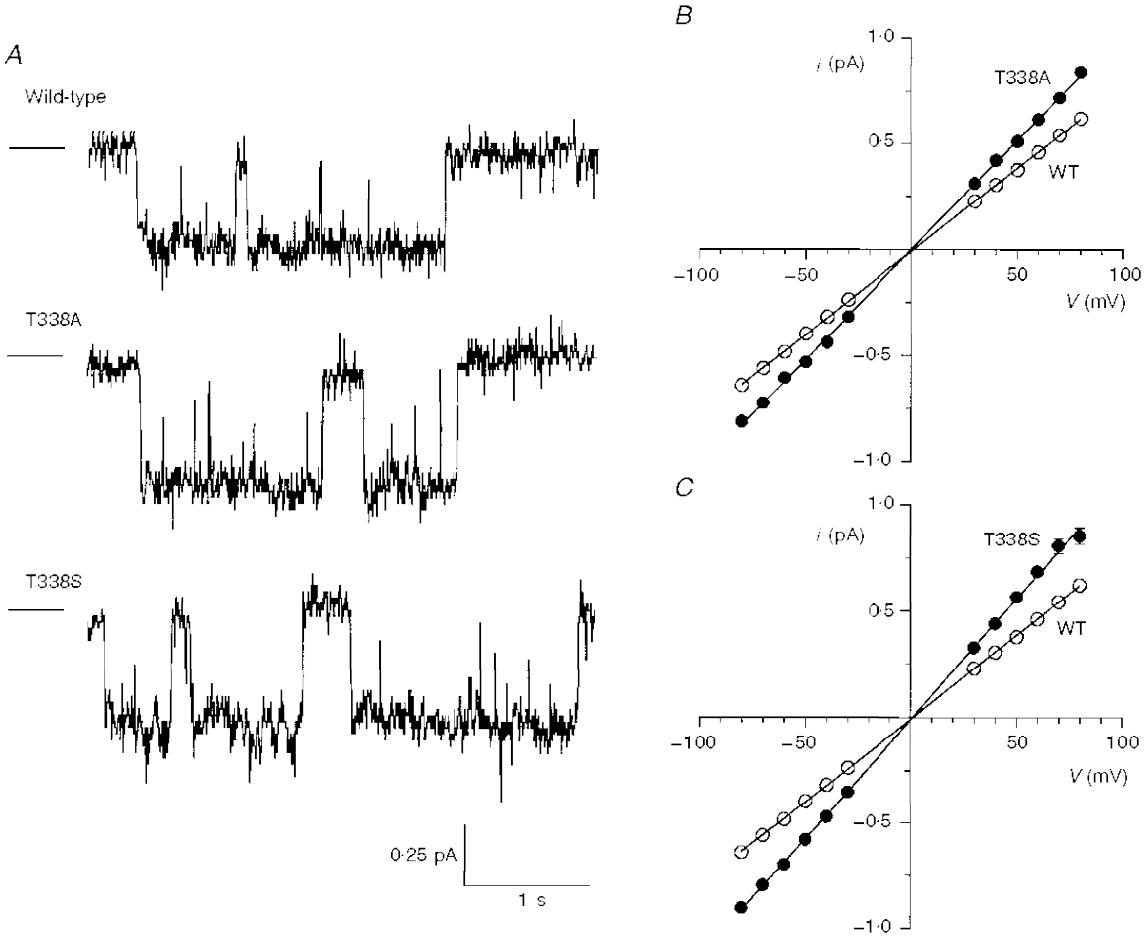

Figure 4. Unitary properties of T338A and T338S CFTR

A, examples of single channel activity for wild-type, T338A and T338S, recorded at −50 mV. In each case the line to the left represents the closed state of the channel. *B* and *C*, mean single channel current–voltage relationships for wild-type, T338A (*B*) and T338S (*C*). Mean of data from five to eighteen patches.

In contrast to wild-type, activation of macroscopic T338I (Fig. 5*C* and *D*) and T338N and T338V (data not shown) Cl^- currents was associated with only a very small increase in noise. Analysis of current variance (e.g. Fig. 5*D*) yielded chord conductances at −50 mV of 0·23 ± 0·02 pS ($n = 4$) for T338N, 0·36 ± 0·10 pS ($n = 5$) for T338V, and 0·17 ± 0·04 pS ($n = 5$) for T338I. Although, as for wild-type (see above), these values may be underestimates, they are consistent with our inability to resolve unitary currents for any of these mutants.

The effect of mutating T338 on unitary Cl^- conductance was correlated with the size of the amino acid side chain substituted at this position (Fig. 6). Thus, those amino acids with smaller side chains than threonine (i.e. alanine and serine) showed significantly increased conductance compared with wild-type (see above). Conversely, substitution of larger amino acids (asparagine, valine, isoleucine) resulted in channels with extremely low conductance (Fig. 6). Phenylalanine had the largest side chain volume of all amino acids substituted (approximately 0·093 nm^3; Richards, 1974). Thus, the lack of macroscopic Cl^- currents in membrane patches excised from BHK cells expressing T338F (see above) may reflect a non-conducting phenotype for this mutant. Alternatively, misprocessing or degradation of T338F protein (Fig. 1*C*) may result in expression levels below our threshold of detection using patch clamp recording.

Anion selectivity of T338 mutants

The ionic selectivity of macroscopic currents carried by T338 mutant channels was examined in inside-out patches by replacing intracellular Cl^- with other anions under biionic conditions (see Methods), as described previously for wild-type CFTR (Linsdell & Hanrahan, 1998). T338I gave only very small currents when intracellular Cl^- was replaced by other anions, such that accurate measurement of V_{rev} was not possible, and therefore the selectivity of this mutant was not studied further. Anion selectivity was greatly altered in all T338 mutants studied, as illustrated by

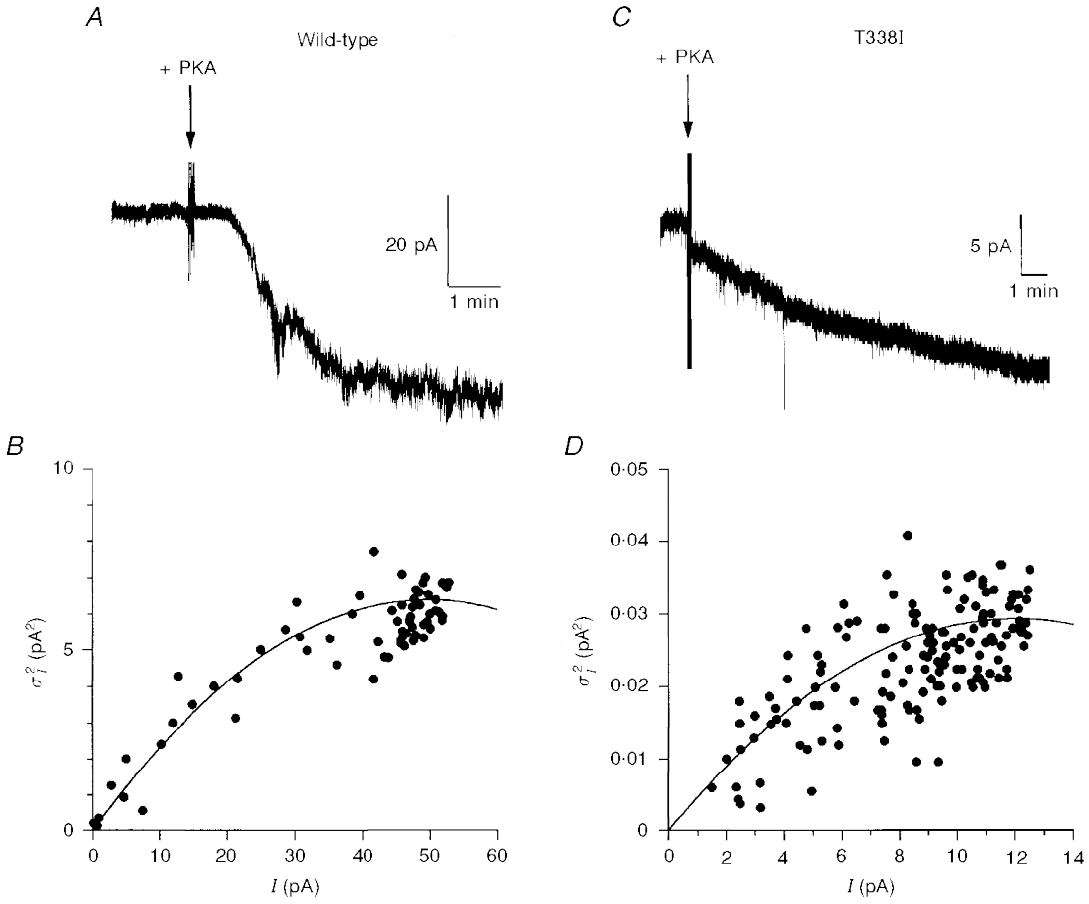

Figure 5. Estimation of unitary current amplitude from macroscopic current noise

A and *C*, activation of macroscopic CFTR current at −50 mV is associated with a large increase in current noise for wild-type (*A*), but a much smaller increase in noise for T338I (*C*). Note the different current scales used in *A* and *C*. Addition of protein kinase A catalytic subunit (PKA) is indicated by the arrows. *B* and *D*, relationship between current amplitude (I) and current variance (σ_I^2) for the patches shown in *A* and *C*, respectively, calculated for 5 s subrecords as described in Methods. Note the very different current variance scales in *B* and *D*. In both *B* and *D*, the data have been fitted by eqn (3) (see Methods), giving $i = 0{\cdot}26$ pA and $N = 386$ in *B*, and $i = 0{\cdot}0049$ pA and $N = 4905$ in *D* (i, unitary current; N, total number of channels).

Table 1. Permeability of intracellular anions in wild-type and mutant CFTR Cl^- channels

Anion	WT	T338A	T338S	T338N	T338V	T339V
Thiocyanate	2·63 ± 0·13 (6)	5·85 ± 0·27 (4)*	4·80 ± 0·19 (3)*	8·72 ± 1·03 (4)*	1·92 ± 0·35 (4)*	3·28 ± 0·08 (4)*
Nitrate	1·53 ± 0·04 (7)	2·04 ± 0·08 (3)*	1·82 ± 0·03 (4)*	4·22 ± 0·22 (3)*	6·84 ± 1·18 (7)*	1·61 ± 0·02 (3)
Bromide	1·23 ± 0·03 (5)	1·74 ± 0·04 (3)*	1·47 ± 0·07 (3)*	1·66 ± 0·15 (3)*	1·04 ± 0·09 (5)	1·39 ± 0·06 (4)*
Chloride	1·00 ± 0·01 (10)	1·00 ± 0·02 (11)	1·00 ± 0·02 (6)	1·00 ± 0·03 (10)	1·00 ± 0·04 (11)	1·00 ± 0·06 (10)
Iodide	0·84 ± 0·03 (5)	2·09 ± 0·16 (5)*	1·76 ± 0·09 (3)*	1·03 ± 0·05 (3)*	0·79 ± 0·11 (3)	0·84 ± 0·02 (3)
Perchlorate	0·25 ± 0·02 (6)	1·35 ± 0·08 (3)*	0·66 ± 0·06 (3)*	0·41 ± 0·03 (3)*	0·54 ± 0·00 (3)*	0·24 ± 0·01 (4)
Benzoate	0·069 ± 0·006 (6)	0·17 ± 0·03 (4)*	0·091 ± 0·019 (3)	0·089 ± 0·015 (4)	0·15 ± 0·02 (4)*	0·097 ± 0·014 (4)
Hexa-fluorophosphate	< 0·019 (4)	0·53 ± 0·01 (3)*	0·31 ± 0·02 (3)*	0·68 ± 0·02 (3)*	0·39 ± 0·05 (3)*	0·051 ± 0·010 (4)*
Fluoride	0·11 ± 0·01 (7)	0·12 ± 0·02 (4)	0·095 ± 0·012 (4)	0·11 ± 0·01 (4)	0·093 ± 0·009 (3)	0·17 ± 0·02 (4)*
Formate	0·25 ± 0·01 (8)	0·45 ± 0·04 (3)*	0·43 ± 0·03 (3)*	0·35 ± 0·04 (4)*	0·22 ± 0·01 (3)	0·28 ± 0·02 (3)
Acetate	0·090 ± 0·004 (8)	0·19 ± 0·01 (3)*	0·18 ± 0·01 (3)*	0·10 ± 0·02 (5)	0·11 ± 0·02 (3)	0·16 ± 0·01 (3)*
Propanoate	0·14 ± 0·01 (3)	0·18 ± 0·02 (4)	0·098 ± 0·010 (4)*	0·077 ± 0·013 (3)*	0·13 ± 0·02 (3)	—
Pyruvate	0·10 ± 0·01 (5)	0·20 ± 0·01 (3)*	0·13 ± 0·02 (3)	0·075 ± 0·015 (3)	0·17 ± 0·03 (3)*	—
Methane sulphonate	0·077 ± 0·005 (5)	0·14 ± 0·02 (4)*	0·079 ± 0·014 (3)	0·038 ± 0·004 (3)*	0·088 ± 0·007 (3)	—
Glutamate	0·096 ± 0·008 (4)	0·082 ± 0·009 (3)	0·080 ± 0·008 (3)	0·060 ± 0·012 (5)*	0·11 ± 0·01 (3)	—
Isethionate	0·13 ± 0·01 (4)	0·11 ± 0·01 (3)	0·086 ± 0·012 (5)*	0·043 ± 0·007 (3)*	0·067 ± 0·005 (3)*	—
Gluconate	0·068 ± 0·004 (36)	0·10 ± 0·01 (3)*	0·060 ± 0·004 (3)	0·044 ± 0·004 (3)	0·077 ± 0·009 (3)	0·088 ± 0·021 (5)

Relative permeabilities of different anions present in the intracellular solution under biionic conditions were calculated from macroscopic current reversal potentials (e.g. Figs 7 and 10) as described in Methods. Numbers in parentheses indicate the number of patches examined in each case. * Significantly different from the corresponding value in wild-type ($P < 0·05$, Student's two-tailed t test).

the current–voltage relationships in Fig. 7 and summarized in Table 1. Changes in permeability were greatest for the lyotropic anions SCN^-, NO_3^-, Br^-, I^-, ClO_4^-, PF_6^- and benzoate (Table 1 and Fig. 7). In contrast, the permeability of kosmotropic anions (F^-, formate, acetate, propanoate, pyruvate, methane sulphonate, glutamate, isethionate, gluconate) was generally less strongly affected (Table 1 and Fig. 7). Fluoride permeability was not significantly altered in any T338 mutant (Table 1). Previously, we reported that CFTR shows significant permeability to large intracellular anions, and suggested that this might be a novel function of CFTR (Linsdell & Hanrahan, 1998). The lack of any severe alteration in large anion permeability due to mutation of T338 suggests that these mutations do not strongly disrupt this putative function of CFTR. Cation permeability was negligible in all T338 mutants (data not shown), as we have previously described for wild-type (Linsdell & Hanrahan, 1998).

The alterations in anion permeability observed in T338 mutants were severe enough to change the selectivity sequence. Selectivity sequences for each channel variant are

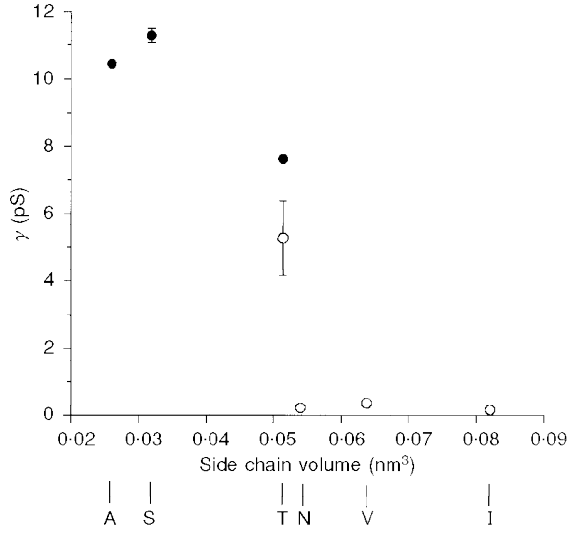

Figure 6. Unitary conductance (γ) of wild-type and T338 mutant CFTRs is related to amino acid side chain size

Conductances were calculated from the slope of single channel current–voltage relationships (●; see Fig. 4) or from the unitary current at −50 mV estimated from macroscopic current variance (○; see Fig. 5). Mean of data from five to eighteen patches (●) or four to five patches (○). The side chain volume of the amino acid residue present at position 338 was estimated according to Richards (1974).

Table 2

Wild-type	$SCN^- > NO_3^- > Br^- > Cl^- > I^- > ClO_4^- >$ formate $> F^- > PF_6^-$
T338A	$SCN^- > I^- \geqslant NO_3^- > Br^- > ClO_4^- > Cl^- > PF_6^-$ > formate $> F^-$
T338S	$SCN^- > NO_3^- \geqslant I^- > Br^- > Cl^- > ClO_4^-$ > formate $> PF_6^- > F^-$
T338N	$SCN^- > NO_3^- > Br^- > I^- = Cl^- > PF_6^- > ClO_4^-$ > formate $> F^-$
T338V	$NO_3^- > SCN^- > Br^- = Cl^- > I^- > ClO_4^- > PF_6^-$ > formate $> F^-$

shown in Table 2. Note that no two variants shared the same selectivity sequence. All T338 mutants retained the ability to select for lyotropic anions over kosmotropic anions such as F^- and formate. Thus the effects of mutating T338 might best be described as altering selectivity among lyotropic anions without disrupting selectivity against kosmotropic anions.

Among lyotropic anions, the selectivity sequences obtained for different channel variants are shown in Table 3. Note that all lyotropic anions showed the permeability sequence T338A > T338S > wild-type, again suggesting that the effects of these mutations on pore properties are correlated with the size of the amino acid side chain substituted. However, the permeabilities of the low conductance mutants T338N and T338V were more difficult to interpret, possibly indicating that substitution of a larger amino acid for T338 causes a more severe disruption of pore function. These sequences also demonstrate that the general effect of mutating T338 was to increase the permeability of lyotropic anions, since wild-type (T) comes at or near the bottom of each selectivity sequence.

Pore diameter of T338 mutants

Previously, we suggested that the double mutant channel, TT338,339AA, had an increased minimum functional pore diameter, based on its increased permeability to extracellular formate, acetate, propanoate and pyruvate ions (Linsdell *et*

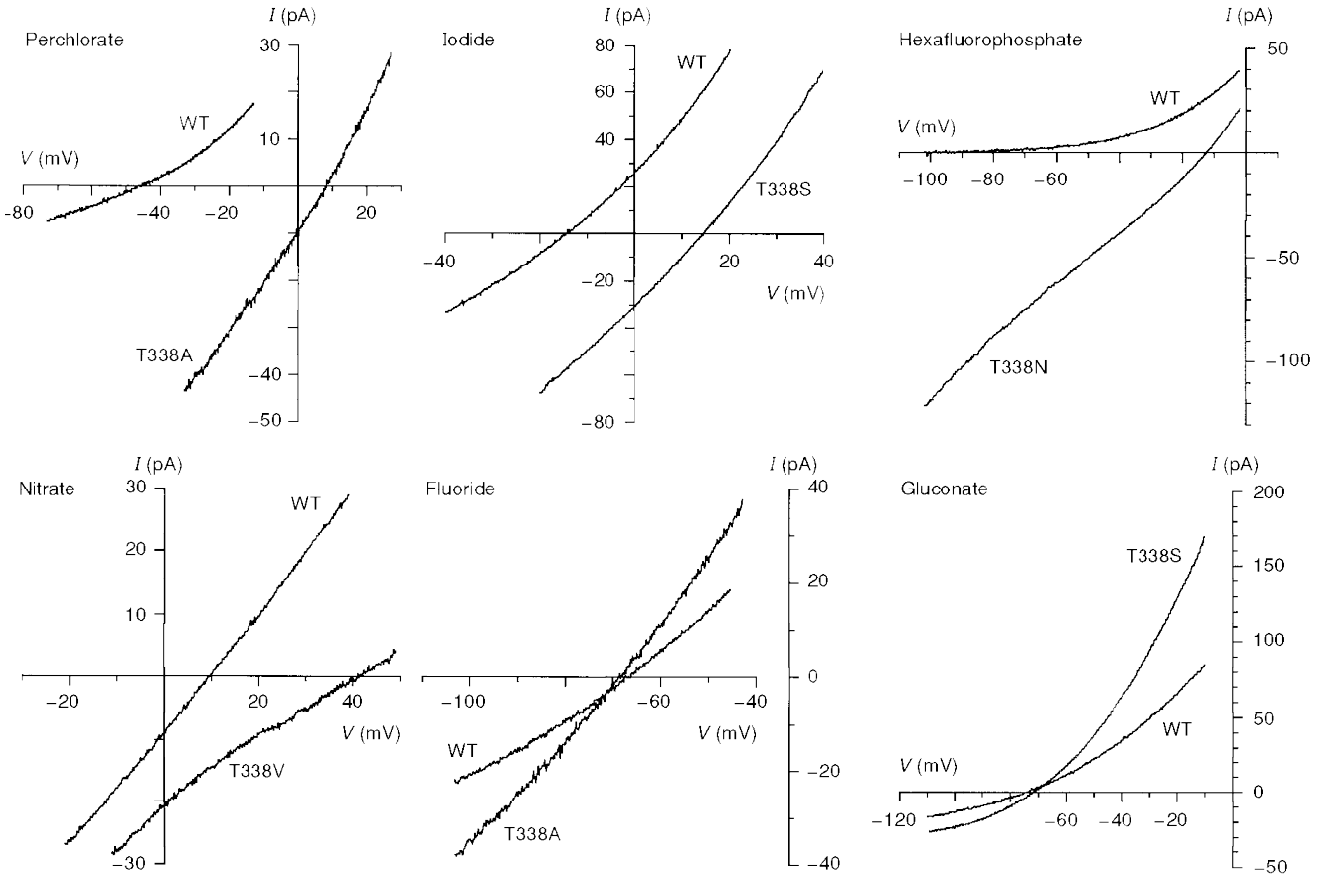

Figure 7. Example current–voltage relationships recorded under biionic conditions with the named anion substituted for Cl^- in the intracellular solution

The differences in reversal potential between wild-type and different T338 mutants reflect large underlying changes in anion selectivity. Patches were held at 0 mV and depolarizing voltage ramps were applied at a rate of 37·5–62·5 mV s^{-1}. Current–voltage relationships were leak subtracted as described in Methods.

Table 3

SCN^-	N > A > S > T > V
NO_3^-	V > N > A > S > T
Br^-	A > N > S > T > V
I^-	A > S > N > T = V
PF_6^-	N > A > V > S > T

Single letters correspond to the amino acid residue present at position 338.

al. 1997*b*). The substitution of amino acids with side chains both smaller and larger than that of the wild-type threonine at position 338 allowed us to examine more fully the role of this residue in contributing to a physical constriction in the CFTR pore.

The asymmetrical permeability of large organic anions in CFTR means that very different functional pore diameters are estimated using different ionic conditions (Linsdell & Hanrahan, 1998). These results underline the fact that the apparent pore diameter estimated in this way is a functional, rather than a physical, parameter. However, for wild-type CFTR, similar estimates of functional pore diameter (approximately 0·53 nm) were obtained by studying the relationship between the ionic diameter and permeability of both intracellular lyotropic anions and extracellular kosmotropic anions (Linsdell *et al.* 1997*b*; Linsdell & Hanrahan, 1998). This contrasts with a value of approximately 0·58 nm for the TT338,339AA mutant under similar conditions (Linsdell *et al.* 1997*b*). The relationships between the permeability of intracellular lyotropes (Table 1) and their mean unhydrated diameters (taken from Linsdell & Hanrahan, 1998) are shown in Fig. 8. In each case the data have been fitted by eqn (2), giving minimum functional pore diameters of 0·528 nm (wild-type), 0·576 nm (T338A), 0·549 nm (T338S), 0·510 nm (T338N) and 0·540 nm (T338V). These small changes in apparent pore diameter are

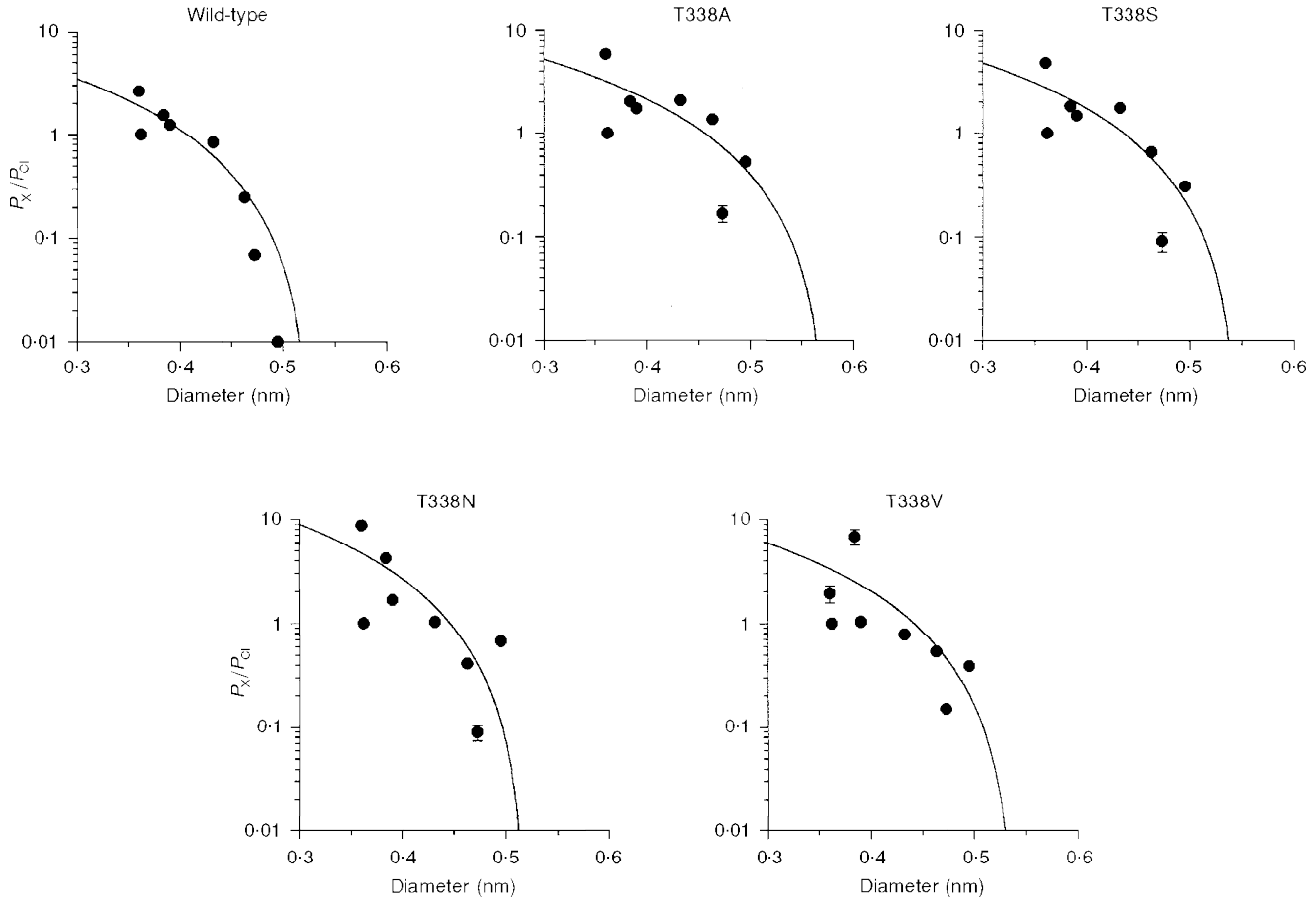

Figure 8. Relationship between the permeability of intracellular lyotropic anions and their mean diameters, in wild-type and T338 mutant CFTRs

Permeability ratios (P_X/P_{Cl}) for SCN^-, NO_3^-, Br^-, Cl^-, I^-, ClO_4^-, benzoate and PF_6^- were taken from Table 1; ionic diameters are as calculated previously (Linsdell & Hanrahan, 1998). In each case the data have been fitted using eqn (2) (see Methods), giving estimates of the functional pore diameter (d) of 0·528 nm for wild-type, 0·576 nm for T338A, 0·549 nm for T338S, 0·510 nm for T338N and 0·540 nm for T338V. Anions examined (in order of increasing diameter) were: SCN^-, Cl^-, NO_3^-, Br^-, I^-, ClO_4^-, benzoate and PF_6^-.

probably not significant considering that the permeability of the largest lyotropic anions studied (PF_6^-, benzoate and ClO_4^-) were increased in all T338 mutants, irrespective of the side chain size of the amino acid substituted.

We also examined the permeability of the organic anions formate, acetate, propanoate, pyruvate, methane sulphonate and gluconate from the extracellular side of the membrane for each T338 mutant (Fig. 9). In this case, fits by eqn (2) suggested minimum pore diameters of 0·535 nm (wild-type), 0·615 nm (T338A), 0·505 nm (T338S), 0·503 nm (T338N) and 0·530 nm (T338V). Again, these results do not suggest a strong relationship between the size of the amino acid side chain present at position 338 (see Fig. 6) and functional pore diameter, arguing against a direct role for T338 in contributing to the narrowest part of the pore.

Effects of mutations at T339

Of five amino acid substitutions carried out at position 339, only one (T339V) resulted in the production of detectable amounts of CFTR protein (Fig. 1*D*). Indeed, we found no PKA- and ATP-dependent currents in very large inside-out patches excised from BHK cells expressing T339A ($n = 6$), T339S ($n = 4$), T339Y ($n = 6$) or T339F ($n = 5$) using symmetrical 150 mM NaCl-containing solutions (not shown). PKA- and ATP-dependent currents were observed, however, in twelve of fourteen T339V CFTR patches under the same conditions (Fig. 10*A*). T339V showed slight inward current rectification under these symmetrical ionic conditions ($-I_{+50}/I_{-50} = 0{\cdot}86 \pm 0{\cdot}01$; $n = 8$). This inward rectification was also observed at the single channel level (Fig. 11), with unitary currents being smaller than wild-type at depolarized, but not hyperpolarized, potentials. Mean chord conductances for T339V were $7{\cdot}95 \pm 0{\cdot}16$ pS ($n = 4$) at −50 mV and $6{\cdot}37 \pm 0{\cdot}29$ pS ($n = 3$) at +50 mV, compared with wild-type values of $7{\cdot}91 \pm 0{\cdot}09$ pS ($n = 18$) at −50 mV and $7{\cdot}85 \pm 0{\cdot}09$ pS ($n = 12$) at +50 mV. As with T338A and T338S, T339V showed apparently normal channel gating, with open probability being time and

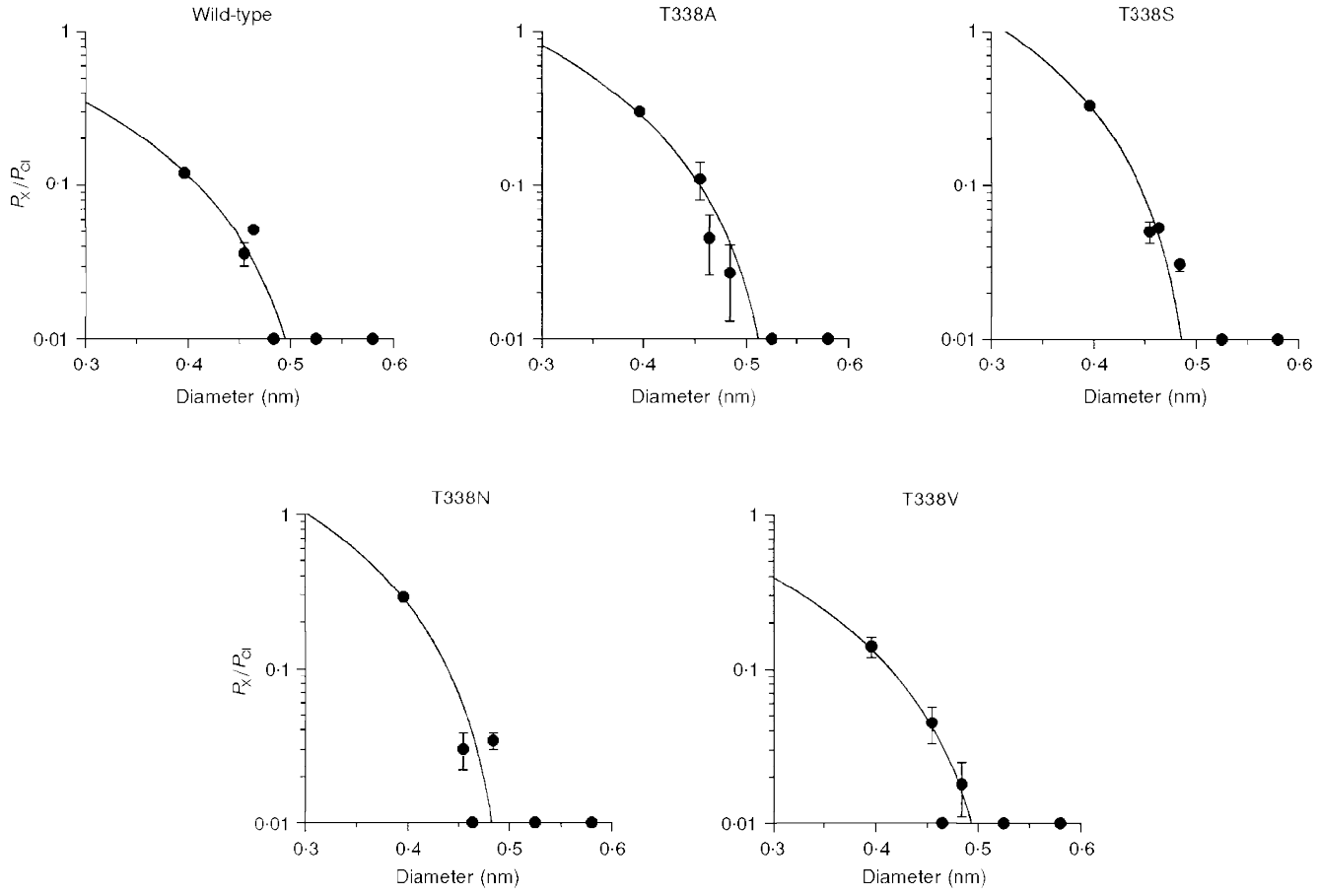

Figure 9. Relationship between the permeability of extracellular organic (kosmotropic) anions and their mean diameters, in wild-type and T338 mutant CFTRs

Permeability ratios (P_X/P_{Cl}) for formate, acetate, propanoate, pyruvate, methane sulphonate and gluconate were taken from Table 1; their ionic diameters are as calculated previously (Linsdell & Hanrahan, 1998). In each case the data have been fitted using eqn (2) (see Methods), giving estimates of the functional pore diameter (d) of 0·535 nm for wild type, 0·615 nm for T338A, 0·505 nm for T338S, 0·503 nm for T338N and 0·530 nm for T338V. Anions examined (in order of increasing diameter) were: formate, acetate, propanoate, pyruvate, methane sulphonate and gluconate.

voltage independent. Furthermore, as with T338 mutants, T339V had negligible cation permeability (data not shown).

The T339V mutant also had significant alterations in ionic permeability (Fig. 10*B* and Table 1), although in general these were not as strong as those observed for T338 mutants. Indeed, the selectivity sequence for T339V ($SCN^- > NO_3^- > Br^- > Cl^- > I^- > ClO_4^- >$ formate $> F^- > PF_6^-$) was the same as for wild-type (see Table 2). Gluconate permeability was not significantly altered in T339V, again suggesting no severe disruption of large organic anion permeability. All of these effects are consistent with the T339V mutant having less severely altered pore properties than any of the T338 mutants studied.

DISCUSSION

T338 and CFTR permeation properties

Mutagenesis of a number of different amino acid residues in the TM6 region of the CFTR pore alters permeation properties such as unitary conductance and anion binding (Anderson *et al.* 1991; Sheppard *et al.* 1993; Tabcharani *et al.* 1993; McDonough *et al.* 1994; Linsdell & Hanrahan, 1996; Linsdell *et al.* 1997*b*; Mansoura *et al.* 1998). In addition, the finding that amino acid side chains throughout and flanking TM6 line the aqueous lumen of the pore (Cheung & Akabas, 1996) supports a key role for this region in forming the permeation pathway for anions. Other membrane-spanning regions presumably also contribute to the pore (e.g. McDonough *et al.* 1994; Mansoura *et al.* 1998), although so far these regions have received less attention than TM6. We have shown that mutation of TM6 residue T338, the side chain of which does not appear to line the pore (Cheung & Akabas, 1996; see below), strongly affects the conductance and selectivity of the CFTR Cl^- channel.

All amino acid substitutions carried out for T338 strongly affected unitary Cl^- conductance, with both increases and decreases in conductance being observed depending on the amino acid substituted (Figs 4 and 6). The conductance of different T338 mutants varied over almost two orders of magnitude (Fig. 6), although the low conductances estimated for T338N, T338V and T338I should be considered rough approximations only. The very low apparent conductances of these three mutants is reminiscent of the effect of mutating a nearby TM6 residue, S341 (McDonough *et al.* 1994). The central portion of TM6 containing both of these key amino acids (T338 and S341) may therefore be the region where conductance is mainly determined. The low conductance of T338I could also explain why this mutation is associated with CF (Saba *et al.* 1993), although partial misprocessing (Fig. 1*C*) may also play a role. Conversely, the elevated conductance of T338A and T338S might be advantageous in gene or protein replacement therapies for

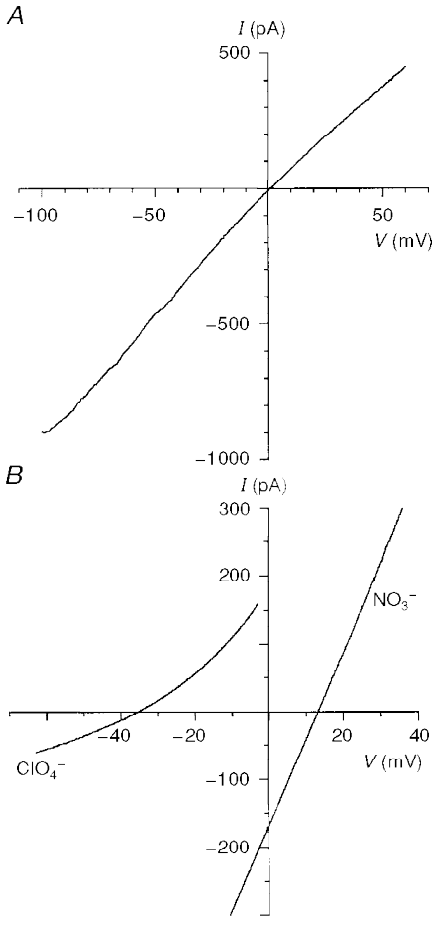

Figure 10. Macroscopic current–voltage relationships for T339V CFTR

A, T339V shows slight inward rectification with symmetrical Cl^--containing solutions. *B*, example current–voltage relationships used to investigate the anion selectivity of T339V, measured under biionic conditions with ClO_4^- or NO_3^- in the intracellular solution. Note that the permeability of these ions in T339V is similar to that observed in wild-type (Fig. 7). Patches were held at 0 mV and depolarizing voltage ramps were applied at a rate of 37·5–100 mV s^{-1}. Current–voltage relationships were leak subtracted as described in Methods.

CF, as we previously suggested for the double mutant TT338,339AA (Linsdell *et al.* 1997*b*). Since Cl^- is the only lyotropic anion found in biological fluids (Collins, 1997), the altered selectivity of these mutants is unlikely to have any adverse effects. Furthermore, permeation by large intracellular anions, which we previously suggested might have an important physiological role (Linsdell & Hanrahan, 1998), is not disrupted in these mutants. Interestingly, both T338A (10·4 pS; Fig. 4*B*) and T338S (11·3 pS; Fig. 4*C*) have higher conductances than that we reported previously for TT338,339AA (9·9 pS; Linsdell *et al.* 1997*b*). Thus T338S has the highest conductance of any CFTR variant described to date.

All single channel conductances reported in this paper were measured at hyperpolarized potentials; conductance of the mutant channels T338N, T338V and T338I might be significantly lower at depolarized potentials (Fig. 2). The reasons why these mutants show marked inward rectification under symmetrical ionic conditions (Fig. 2) is not clear. Inward rectification is observed in several other TM6 mutants at the single channel level, e.g. K335E (Tabcharani *et al.* 1993), T339V (Fig. 11*B*) and I332K (P. Linsdell, J. A. Tabcharani & J. W. Hanrahan, unpublished observations); however, voltage-dependent gating in T338 mutants cannot be excluded.

All T338 mutants studied showed strongly altered anion selectivity (Fig. 7 and Table 1). All mutations changed the selectivity sequence among lyotropic anions without disrupting the ability of the channel to select for lyotropic over kosmotropic anions (see Results). The lyotropic anion selectivity sequence of wild-type CFTR suggests that ionic hydration energies are mainly responsible for controlling anion permeability (Linsdell *et al.* 1997*b*; Tabcharani *et al.* 1997). Indeed, there was a strong inverse relationship between permeability and ionic hydration energy (Fig. 12*A*). Obvious deviations from this relationship were the unexpectedly low permeabilities to I^- and ClO_4^- (Fig. 12*A*). The iodide permeability of CFTR has been controversial, with P_I/P_{Cl} values ranging from zero to two having been reported (see Tabcharani *et al.* 1997). In addition, several molecular manipulations of the CFTR protein have previously been reported to alter I^- permeability (Anderson *et al.* 1991; Price *et al.* 1996; Sheppard *et al.* 1996; Tabcharani *et al.* 1997; Mansoura *et al.* 1998). Using single channel recording, we have shown that P_I/P_{Cl} can switch spontaneously from 1·8 to $< 0{\cdot}4$ (Tabcharani *et al.* 1997). In the present study we found P_I/P_{Cl} to be 0·84 for wild-type CFTR and 0·79–2·09 for T338 mutants (see Table 1). In no case did P_I/P_{Cl} change with time following patch excision or channel activation with PKA (data not shown), suggesting that no switch in I^- permeability occurs in this system. It remains unclear why the I^- permeability of CFTR shows such variability between different systems.

Low ClO_4^- permeability has previously been reported in CFTR (Gray *et al.* 1993), although very high ClO_4^- permeability has been reported in epithelial outwardly rectifying Cl^- channels (Halm & Frizzell, 1992), volume-regulated Cl^- channels (Verdon *et al.* 1995), and a spontaneously active Cl^- channel from kidney (Shindo *et al.*

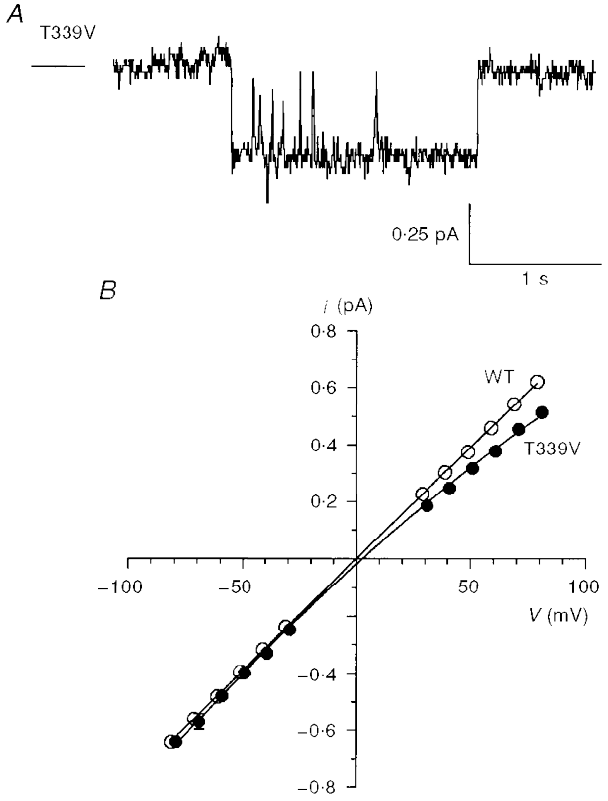

Figure 11. Unitary properties of T339V CFTR
A, activity of a single T339V channel at −50 mV (cf. Fig. 4*A*). *B*, mean single channel current–voltage relationships for wild-type (as in Fig. 4*B* and *C*) and T339V. Mean of data from four to eighteen patches.

1996). One possible explanation for the low ClO_4^- permeability observed might be that movement of this relatively large ion through the pore is limited by stearic factors. However, ClO_4^- permeability was greatly increased in all T338 mutants (Table 1), even though these channels had very similar apparent pore diameters to wild-type (Figs 8 and 9). It may be, therefore, that wild-type CFTR is able to discriminate against both kosmotropic anions (such as F^-) and highly lyotropic anions (such as ClO_4^-). Such a mechanism might suggest that permeating anions interact sequentially with both weak field strength and strong field strength sites within the channel. The increased permeability to lyotropic anions seen in T338 mutants would be consistent with disruption of a site which selects for Cl^- over more lyotropic anions. Thus in T338A, for example, the relationship between permeability and ionic hydration energy appeared much more linear than for wild-type (Fig. 12*B*).

Previously, Cheung & Akabas (1997) suggested that CFTR selectivity for anions over cations is determined at the cytoplasmic end of TM6, possibly in a region which loops back into the channel lumen. Our present results therefore suggest that selectivity between different anions and selectivity for anions over cations are determined by different regions of the CFTR pore.

T339 and CFTR protein processing

In contrast to mutations at T338, most mutations at T339 resulted in reduced expression of CFTR protein (Fig. 1*D* and *E*) and failure to express any detectable PKA- and ATP-dependent current (see Results). Many mutations in CFTR prevent biosynthetic maturation of the protein (e.g. Cheng *et al.* 1990; Gregory *et al.* 1991; Seibert *et al.* 1996). However, it is unclear why mutations at T339 should apparently be more sensitive to misprocessing than those at T338 (Fig. 1*C* and *D*), or why the non-conservative T339V mutation alone should be appropriately processed (Fig. 1*D*). Both T339A (McDonough *et al.* 1994) and T339C (Cheung & Akabas, 1996) mutant channels can be expressed in *Xenopus* oocytes following injection of *in vitro* transcribed cRNA. Furthermore, the double mutant TT338,339AA can be functionally expressed in CHO cells (Linsdell *et al.* 1997*b*), raising the possibility that the detrimental effects of the T339A mutation on processing may be 'rescued' by simultaneous mutation of T338.

Because of low protein expression, we were only able to characterize the permeation properties of one T339 mutant, T339V. This mutant channel showed inward rectification (Fig. 10*A*), reduced unitary conductance at depolarized potentials (Fig. 11*B*), and significant changes in permeability

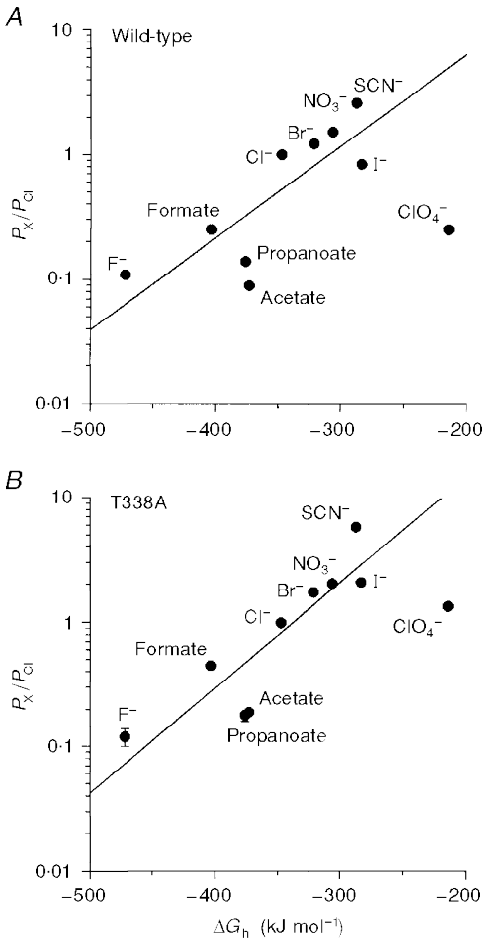

Figure 12. Relationship between relative permeability and free energy of hydration for different intracellular anions

A, wild-type; *B*, T338A. Hydration energies, relative to that of Cl^- (ΔG_h), were taken from Marcus (1997).

(Table 1). However, these effects were less marked than those associated with T338 mutations. Thus T339 may play a similar (although perhaps less important) role as T338 in determining CFTR channel permeation properties. However, the paucity of data concerning the functional effects of mutations at T339 precludes any strong conclusions regarding its role in pore structure.

Functional diameter of the CFTR channel pore

An interesting effect of the TT338,339AA double mutation was an apparent increase in the functional diameter of the CFTR channel pore, manifested as an increase in permeability to extracellular formate, acetate, propanoate and pyruvate ions (Linsdell *et al.* 1997*b*). However, in this study we found that substitution of the native T338 by larger or smaller amino acid residues did not strongly affect the functional minimum pore diameter (Figs 8 and 9). Thus our present results do not support a major role for T338 in contributing to the narrow pore region. Although it remains a possibility that T339 contributes to a constriction in the pore, the effects of replacing T339 with a larger valine residue on the permeability to large anions (significantly increased permeability to PF_6^- and acetate, similar permeability to ClO_4^-, benzoate, formate and gluconate; Table 1) do not suggest that it limits functional pore diameter. Our recent finding that the pore of wild-type CFTR may be able to adopt a much wider conformation than that suggested by Figs 8 and 9 (Linsdell & Hanrahan, 1998) emphasises that the minimum pore diameter estimated in this way is a functional rather than a physical parameter. It is possible that both T338 and T339 are located near a physical constriction in the pore, and that simultaneous mutagenesis of both residues is necessary to influence functional pore diameter. The relationship between channel conductance and the size of the amino acid side chain present at residue 338 (Fig. 6; see below) is consistent with this residue being located in a physically restricted part of the pore.

Structural implications for the CFTR pore

The effects of mutating T338 on channel conductance (Fig. 6) and selectivity (Table 1; see also Results) seem to be correlated with the size of the amino acid side chain at this position. In contrast, no strong correlation with the nature of the side chain substituted was obvious. These size-related effects, together with the report that the side chain of residue 338 does not line the aqueous lumen of the pore (Cheung & Akabas, 1996), suggests that mutations at T338 may alter pore properties via an indirect effect on the orientation of the TM6 helix. Such an allosteric effect could alter an anion binding site contributed by nearby amino acid side chains or the peptide backbone. It has previously been suggested that the amide nitrogen of the peptide backbone may interact preferentially with lyotropic anions (see Collins, 1997). Participation of the peptide backbone in forming an anion selectivity filter might explain why different classes of Cl^- channels, which share no significant homology (Jentsch & Günther, 1997), show such similar anion selectivity (see Introduction). The diverse molecular structures of Cl^- channel types suggest that there is no unique Cl^- channel 'signature sequence' of amino acid residues, such as that which occurs in all known K^+ channel pores (Heginbotham *et al.* 1994). A conserved amino acid sequence (GKxGPxxH) does contribute to anion selectivity in the ClC family of Cl^- channels (Fahlke *et al.* 1997); however, this sequence is not found in CFTR. In contrast, a common arrangement of the peptide backbone, possibly in conjunction with nearby hydrophobic amino acid side chains (see below), could provide a common structural element in unrelated Cl^- channel pores. Interestingly, the recently described crystal structure of a *Streptomyces lividans* K^+ channel (Doyle *et al.* 1998) indicates that the peptide backbone lines the narrow region of the pore where selectivity is determined.

The pore of the gramicidin channel is lined only by the peptide backbone, and yet shows ideal selectivity for cations over anions (Dorman *et al.* 1996; Roux, 1996). For the peptide backbone to contribute to a lyotropic selectivity filter in the pore of an anion selective channel, therefore, would presumably require a specific orientation or local environment quite different from that found in the gramicidin channel. Anion binding to model compounds is thought to follow the lyotropic sequence when a cationic group or dipole attracts anions into water structured around hydrophobic groups (see Dani *et al.* 1983). Thus the amide nitrogen of the peptide backbone may be able to form a lyotropic anion attracting group only if it is in close proximity to one or more hydrophobic amino acid side chains.

Although threonine has a polar, hydrophilic side chain, it is often buried in the water-inaccessible face of transmembrane helices (Gray & Matthews, 1984). Indeed, this it thought to be the case for both T338 and T339 (Cheung & Akabas, 1996). Under these conditions, buried threonine residues are thought to form hydrogen bonds with the carbonyl oxygen of the preceding turn of the α-helix (Gray & Matthews, 1984). Threonine residues T338 and T339 might therefore provide structural stability to the TM6 helix of CFTR via intra-helix hydrogen bonding. Mutation of these residues could then disrupt the orientation of the helix, leading to alteration of pore properties (in the case of T338) or misfolding of the protein (in the case of T339).

Anderson, M. P., Gregory, R. J., Thompson, S., Souza, D. W., Paul, S., Mulligan, R. C., Smith, A. E. & Welsh, M. J. (1991). Demonstration that CFTR is a chloride channel by alteration of its anion selectivity. *Science* **253**, 202–205.

Arreola, J., Melvin, J. E. & Begenisich, T. (1995). Volume-activated chloride channels in rat parotid acinar cells. *Journal of Physiology* **484**, 677–687.

Bormann, J., Hamill, O. P. & Sakmann, B. (1987). Mechanism of anion permeation through channels gated by glycine and γ-aminobutyric acid in mouse cultured spinal neurones. *Journal of Physiology* **385**, 243–286.

Chang, X.-B., Tabcharani, J. A., Hou, Y.-X., Jensen, T. J., Kartner, N., Alon, A., Hanrahan, J. W. & Riordan, J. R. (1993). Protein kinase A (PKA) still activates CFTR chloride channel after mutagenesis of all 10 PKA consensus phosphorylation sites. *Journal of Biological Chemistry* **268**, 11304–11311.

Cheng, S. H., Gregory, R. J., Marshall, J., Paul, S., Souza, D. W., White, G. A., O'Riordan, C. R. & Smith, A. E. (1990). Defective intracellular transport and processing of CFTR is the molecular basis of most cystic fibrosis. *Cell* **63**, 827–834.

Cheung, M. & Akabas, M. H. (1996). Identification of cystic fibrosis transmembrane conductance regulator channel-lining residues in and flanking the M6 membrane-spanning segment. *Biophysical Journal* **70**, 2688–2695.

Cheung, M. & Akabas, M. H. (1997). Locating the anion-selectivity filter of the cystic fibrosis transmembrane conductance regulator (CFTR) chloride channel. *Journal of General Physiology* **109**, 289–299.

Collins, K. D. (1997). Charge density-dependent strength of hydration and biological structure. *Biophysical Journal* **72**, 65–76.

Dani, J. A., Sanchez, J. A. & Hille, B. (1983). Lyotropic anions. Na channel gating and Ca electrode response. *Journal of General Physiology* **81**, 255–281.

Dorman, V., Partenskii, M. B. & Jordan, P. C. (1996). A semi-microscopic Monte Carlo study of permeation energetics in a gramicidin-like channel: the origin of cation selectivity. *Biophysical Journal* **70**, 121–134.

Doyle, D. A., Cabral, J. M., Pfuetzner, R. A., Kuo, A., Gulbis, A., Cohen, S. L., Chait, B. T. & MacKinnon, R. (1998). The structure of the potassium channel: molecular basis of K^+ conduction and selectivity. *Science* **280**, 69–77.

Dwyer, T. M., Adams, D. J. & Hille, B. (1980). The permeability of the endplate channel to organic cations in frog muscle. *Journal of General Physiology* **75**, 469–492.

Fahlke, C., Yu, H. T., Beck, C. L., Rhodes, T. H. & George, A. L. Jr (1997). Pore-forming segments in voltage-gated chloride channels. *Nature* **390**, 529–532.

Fatima-Shad, K. & Barry, P. H. (1993). Anion permeation in GABA- and glycine-gated channels of mammalian cultured hippocampal neurons. *Proceedings of the Royal Society* B **253**, 69–75.

Gadsby, D. C., Nagel, G. & Hwang, T.-C. (1995). The CFTR chloride channel of mammalian heart. *Annual Review of Physiology* **57**, 387–416.

Gray, M. A., Plant, S. & Argent, B. E. (1993). cAMP-regulated whole cell chloride currents in pancreatic duct cells. *American Journal of Physiology* **264**, C591–602.

Gray, T. M. & Matthews, B. W. (1984). Intrahelical hydrogen bonding of serine, threonine and cysteine residues within α-helices and its relevance to membrane-bound proteins. *Journal of Molecular Biology* **175**, 75–81.

Gregory, R. J., Rich, D. P., Cheng, S. H., Souza, D. W., Paul, S., Manavalan, P., Anderson, M. P., Welsh, M. J. & Smith, A. E. (1991). Maturation and function of cystic fibrosis transmembrane conductance regulator variants bearing mutations in putative nucleotide-binding domains 1 and 2. *Molecular and Cellular Biology* **11**, 3886–3893.

Halm, D. R. & Frizzell, R. A. (1992). Anion permeation in an apical membrane chloride channel of a secretory epithelial cell. *Journal of General Physiology* **99**, 339–366.

Hanrahan, J. W., Tabcharani, J. A., Becq, F., Mathews, C. J., Augustinas, O., Jensen, T. J., Chang, X.-B. & Riordan, J. R. (1995). Function and dysfunction of the CFTR chloride channel. In *Ion Channels and Genetic Diseases*, ed. Dawson, D. C. & Frizzell, R. A., pp. 125–137. Rockefeller University Press, New York.

Heginbotham, L., Lu, Z., Abramson, T. & MacKinnon, R. (1994). Mutations in the K^+ channel signature sequence. *Biophysical Journal* **66**, 1061–1067.

Jackson, P. S., Churchwell, K., Ballatori, N., Boyer, J. L. & Strange, K. (1996). Swelling-activated anion conductance in skate hepatocytes: regulation by cell Cl^- and ATP. *American Journal of Physiology* **270**, C57–66.

Jentsch, T. J. & Günther, W. (1997). Chloride channels: an emerging molecular picture. *BioEssays* **19**, 117–126.

Li, M., McCann, J. D. & Welsh, M. J. (1990). Apical membrane Cl^- channels in airway epithelia: anion selectivity and effect of an inhibitor. *American Journal of Physiology* **259**, C295–301.

Linsdell, P. & Hanrahan, J. W. (1996). Disulphonic stilbene block of cystic fibrosis transmembrane conductance regulator Cl^- channels expressed in a mammalian cell line and its regulation by a critical pore residue. *Journal of Physiology* **496**, 687–693.

Linsdell, P. & Hanrahan, J. W. (1998) Adenosine triphosphate-dependent asymmetry of anion permeation in the cystic fibrosis transmembrane conductance regulator chloride channel. *Journal of General Physiology* **111**, 601–614.

Linsdell, P., Tabcharani, J. A. & Hanrahan, J. W. (1997*a*). Multi-ion mechanism for ion permeation and block in the cystic fibrosis transmembrane conductance regulator chloride channel. *Journal of General Physiology* **110**, 365–377.

Linsdell, P., Tabcharani, J. A., Rommens, J. M., Hou, Y.-X., Chang, X.-B., Tsui, L.-C., Riordan, J. R. & Hanrahan, J. W. (1997*b*). Permeability of wild-type and mutant cystic fibrosis transmembrane conductance regulator chloride channels to polyatomic anions. *Journal of General Physiology* **110**, 355–364.

Linsdell, P., Zheng, S.-X. & Hanrahan, J. W. (1997*c*). Possible contribution of the peptide backbone to CFTR anion selectivity. *Pediatric Pulmonology* **14**, suppl., 215.

McDonough, S., Davidson, N., Lester, H. A. & McCarty, N. A. (1994). Novel pore-lining residues in CFTR that govern permeation and open-channel block. *Neuron* **13**, 623–634.

Mansoura, M. K., Smith, S. S., Choi, A. D., Richards, N. W., Strong, T. V., Drumm, M. L., Collins, F. S. & Dawson, D. C. (1998). Cystic fibrosis transmembrane conductance regulator (CFTR) anion binding as a probe of the pore. *Biophysical Journal* **74**, 1320–1332.

Marcus, Y. (1997). *Ion Properties*. Marcel Dekker, New York.

Price, M. P., Ishihara, H., Sheppard, D. N. & Welsh, M. J. (1996). Function of *Xenopus* cystic fibrosis transmembrane conductance regulator (CFTR) Cl^- channels and use of human–*Xenopus* chimeras to investigate the pore properties of CFTR. *Journal of Biological Chemistry* **271**, 25184–25191.

Richards, F. M. (1974). The interpretation of protein structures: total volume, group volume distributions and packing density. *Journal of Molecular Biology* **82**, 1–14.

Riordan, J. R., Rommens, J. M., Kerem, B., Alon, N., Rozmahel, R., Grzelczak, Z., Zielenski, J., Lok, S., Plasvik, N., Chou, J.-L., Drumm, M. L., Iannuzzi, M. C., Collins, F. S. & Tsui, L.-C. (1989). Identification of the cystic fibrosis gene: cloning and characterization of complementary DNA. *Science* **245**, 1066–1073.

Roux, B. (1996). Valence selectivity of the gramicidin channel: a molecular dynamics free energy perturbation study. *Biophysical Journal* **71**, 3177–3185.

Saba, L., Leoni, G. B., Meloni, A., Faà, V., Cao, A. & Rosatelli, M. C. (1993). Two novel mutations in the transmembrane domains of the CFTR gene in subjects of Sardinian descent. *Human Molecular Genetics* **2**, 1739–1740.

Seibert, F. S., Linsdell, P., Loo, T. W., Hanrahan, J. W., Clarke, D. M. & Riordan, J. R. (1996). Disease-associated mutations in the fourth cytoplasmic loop of cystic fibrosis transmembrane conductance regulator compromise biosynthetic processing and chloride channel activity. *Journal of Biological Chemistry* **271**, 15139–15145.

Sheppard, D. N., Rich, D. P., Ostedgaard, L. S., Gregory, R. J., Smith, A. E. & Welsh, M. J. (1993). Mutations in CFTR associated with mild-disease-form Cl^- channels with altered pore properties. *Nature* **362**, 160–164.

Sheppard, D. N., Travis, S. M., Ishihara, H. & Welsh, M. J. (1996). Contribution of proline residues in the membrane-spanning domains of cystic fibrosis transmembrane conductance regulator to chloride channel function. *Journal of Biological Chemistry* **271**, 14995–15001.

Shindo, M., Simmons, N. L. & Gray, M. A. (1996). Characterization of whole cell chloride conductances in a mouse inner medullary collecting duct cell line mIMCD-3. *Journal of Membrane Biology* **149**, 21–31.

Tabcharani, J. A., Chang, X.-B., Riordan, J. R. & Hanrahan, J. W. (1991). Phosphorylation-regulated Cl^- channel in CHO cells stably expressing the cystic fibrosis gene. *Nature* **352**, 628–631.

Tabcharani, J. A., Linsdell, P. & Hanrahan, J. W. (1997). Halide permeation in wild-type and mutant cystic fibrosis transmembrane conductance regulator chloride channels. *Journal of General Physiology* **110**, 341–354.

Tabcharani, J. A., Rommens, J. M., Hou, Y.-X., Chang, X.-B., Tsui, L.-C., Riordan, J. R. & Hanrahan, J. W. (1993). Multi-ion pore behaviour in the CFTR chloride channel. *Nature* **366**, 79–82.

Verdon, B., Winpenny, J. P., Whitfield, K. J., Argent, B. E. & Gray, M. A. (1995). Volume-activated chloride currents in pancreatic duct cells. *Journal of Membrane Biology* **147**, 173–183.

Acknowledgements

We thank Dr Johanna Rommens for providing pNUT–CFTR cDNA, Drs Norbert Kartner and John Riordan and Mr Tim Jensen for M3A7 antibody to CFTR, Drs Fabian Seibert and Tang Zhu for assistance with transfections and Western blotting, and Jie Liao for maintaining the cell cultures. This work was supported by the Canadian Medical Research Council (MRC), Canadian Cystic Fibrosis Foundation (CCFF), and National Institutes of Health (NIDDK). P.L. is a CCFF postdoctoral fellow. J.W.H. is an MRC scientist.

Corresponding author

P. Linsdell: Department of Physiology, McGill University, 3655 Drummond Street, Montréal, Québec, Canada H3G 1Y6.

Email: linsdell@physio.mcgill.ca